Inorganic Chemistry
Article

Inorg. Chem. **2010**, *49*, 3261–3270 **3261**
DOI: 10.1021/ic902176e

Impact of the Carbon Chain Length of Novel Palladium(II) Complexes on Interaction with DNA and Cytotoxic Activity

Enjun Gao,* Mingchang Zhu, Lei Liu, Yun Huang, Lei Wang, Chuyue Shi, Wanzhong Zhang, and Yaguang Sun

Laboratory of Coordination Chemistry, Shenyang University of Chemical Technology, Shenyang 110142, People's Republic of China

Received November 4, 2009

A series of Pd(II) complexes with a benzenealkyl dicarboxlate chain, with the formulas $[Pd(L_n)(bipy)]\cdot mH_2O$ (bipy = 2,2′-bipyridine, complex **1**: L_1 = phenylmalonate, m = 2.5; complex **2**: L_2 = benzylmalonate, m = 1; complex **3**: L_3 = phenethylmalonate, m = 2; complex **4**: L_4 = phenylpropylmalonate, m = 5), have been prepared in an attempt to correlate factors about the carbon chain of the compounds with DNA binding and cytotoxic activity. The binding of complexes with fish sperm DNA (FS-DNA) was carried out by UV absorption and fluorescence spectra. A gel electrophoresis assay demonstrated the ability of the complexes to cleave the pBR322 plasmid DNA. The cytotoxic effects of these complexes were examined on four cancer cell lines, HeLa, Hep-G2, KB, and AGZY-83a. The four complexes exhibited cytotoxic specificity and a significant cancer cell inhibitory rate. An apparent dependence of DNA-binding properties and cytotoxicity on the carbon chain length was obtained: the longer the carbon chain length, the higher the efficiency of DNA-binding and the greater the cytotoxicity.

1. Introduction

One of the most rapidly developing areas of pharmaceutical research is the discovery of drugs for cancer therapy. Cisplatin (*cis*-diamminedichloroplatinum(II)) is a widely used and well-known metal-based drug for cancer therapy, but it possesses inherent limitations because of the development of resistance in tumor cells and serious side effects such as nausea and kidney and liver failure typical of heavy metal toxicity.[1−7] Anyway, the success of cisplatin in anticancer chemotherapy has raised great interest in the study of metal complexes with low toxicity and improved therapeutic properties to be used as antitumor agents, instigating the ongoing investigation of alternative metal-based drugs.[8,9] In this situation, treatment of cancer with a sequence of chemically different active metallocomplexes is desirable and provides an incentive for expanded research to discover a greater variety of new metal compounds.[10−14]

On the basis of the structural and thermodynamic analogy between platinum(II) and palladium(II) complexes,[15−19] there is also much interest in the design and synthesis of palladium(II) derivatives capable of interacting with biomolecules producing a pharmacological action.[20] Furthermore, some mixed ligand palladium(II) complexes have been shown to act as potential anticancer agents.[21−29]

Farrell and co-workers have reported a series of binuclear platinum complexes bridged by an aliphatic diamine as a

*To whom correspondence should be addressed. Tel.: +86 24 89385016. Fax: +86 24 89388211. E-mail: ejgao@yahoo.com.cn.

(1) Boulikas, T.; Vougiouka, M. *Oncol. Rep.* **2003**, *10*, 1663–1682.
(2) Wong, E.; Giandomenico, C. M. *Chem. Rev.* **1999**, *99*, 2451–2466.
(3) Galanski, M.; Arion, V. B.; Jakupec, M. A.; Keppler, B. K. *Curr. Pharm. Des.* **2003**, *9*, 2078–2089.
(4) Tanaka, T.; Yukawa, K.; Umesaki, N. *Oncol. Rep.* **2005**, *14*, 1365–1369.
(5) Wang, D.; Lippard, S. J. *Nat. Rev. Drug Discovery* **2005**, *4*, 307–320.
(6) Berners-Price, S. J.; Appleton, T. G. In *Platinum-Based Drugs in Cancer Therapy*; Kelland, L. R., Farrell, N., Eds.; Humana Press: Totowa, NJ, 2000; pp 3−31.
(7) Angeles-Boza, A. M.; Bradley, P. M.; Fu, P. K.-L.; Wicke, S. E.; Bacsa, J.; Dunbar, K. M.; Turro, C. *Inorg. Chem.* **2004**, *43*, 8510–8519.
(8) Sherman, S. E.; Lippard, S. J. *Chem. Rev.* **1987**, *87*, 1153–118.
(9) Reedijk, J. *P. Appl. Chem.* **1987**, *59*, 181–186.
(10) Hegmans, A.; Qu, Y.; Kelland, L. R.; Roberts, J. D.; Farrell, N. *Inorg. Chem.* **2001**, *40*, 6108–6114.
(11) Hall, M. D.; Failes, T. W.; Hibbs, D. E.; Hambley, T. W. *Inorg. Chem.* **2002**, *41*, 1223–1228.
(12) Canete, M.; Ortiz., A.; Juarranz, A.; Villanueva, A.; Nonell, S.; Borrell, J. I.; Teixido, J.; Stockert, J. C. *Anti-Cancer Drug Des.* **2000**, *15*, 1143–156.
(13) Kaminskaya, N. V.; Ullmann, M. G.; Fulton, D. B.; Kostic, N. M. *Inorg. Chem.* **2000**, *39*, 5004–5013.
(14) Davies, M. S.; Thomas, D. S.; Hegmans, A.; Berners-Price, S.; Farrell, N. *Inorg. Chem.* **2002**, *41*, 1101–1109.
(15) Rau, T.; van Eldik, R. In *Metal Ions in Biological Systems*; Sigel, A., Sigel, H., Eds.; Marcel Dekker: New York, 1996; Vol. *32*, p 339.
(16) Micklitz, W.; Sheldrick, W. S.; Lippert, B. *Inorg. Chem.* **1990**, *29*, 211–216.
(17) Barnham, K. J.; Bauer, C. J.; Djuran, M. I.; Mazid, M. A.; Rau, T.; Sadler, P. J. *Inorg. Chem.* **1995**, *34*, 2826–2832.
(18) Shen, W. Z.; Gupta, D.; Lippert, B. *Inorg. Chem.* **2005**, *44*, 8249–8258.
(19) Cisplatin. *Chemistry and Biochemistry of a Leading Anticancer Drug*; Lippert, B., Ed.; Wiley-VCH: Weinheim, Germany, 1999.
(20) Al-Allaf, T. A.; Rashan, L. *J. Boll. Chim. Farmac.* **2001**, *140*, 205–210.

Published on Web 03/03/2010

Scheme 1. Reacting Route of the Four Complexes

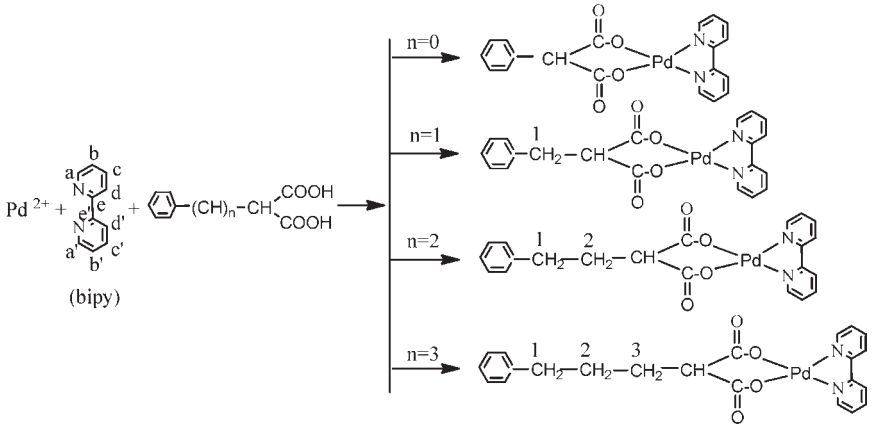

unique class of potential anticancer agents.[30,31] In the present study, we report the synthesis, structures, characterization, cytotoxic activity, interactions with fish sperm DNA (FS-DNA), cleavage behavior toward pBR322 DNA, and in vitro cytotoxic and antiproliferative activity of novel palladium(II) compounds derived from a benzenealkyl dicarboxlate chain group (Scheme1), with the general formulas $[Pd(L_n)(bipy)]\cdot mH_2O$ (bipy = 2,2′-bipyridine, complex **1**: L_1 = phenylamlonate, m = 2.5; complex **2**, previously reported by ourselves:[32] L_2 = benzylmalonate, m = 2; complex **3**: L_3 = phenethylmalonate, m = 2; complex **4**: L_4 = phenylpropylmalonate, m = 5). The influence of the carbon chains bound to a Pd(II) center on the behavior of the structures, DNA interaction, and cytotoxic activity was also investigated.

2. Experimental Section

2.1. Materials and Physical Measurements. $[K_2PdCl_4]$ was synthesized with $PdCl_2$ and KCl by ourselves. The ligands L_3 and L_4 were prepared according to a previously published method with some modifications.[33] Other chemicals and reagents were of reagent grade and used without further purification. The pBR322 plasmid DNA was purchased from the Sino-American Biotechnology Company. The HeLa (human cervix epitheloid carcinoma) cells, the Hep-G2 (human hepatocellular carcinoma) cells, the KB (human oral epithelial carcinoma) cells, and the AGZY-83a (human lung carcinoma) cells were obtained from the American Type Culture Collection.

Elemental analysis (C, H, and N) was performed on a model Finnigan EA 1112. The IR spectra were run as KBr pellets on a Nicolet IR-470. The ^1H and ^{13}C NMR spectra were recorded on a DRX 500 Bruker spectrometer at 298 K with TMS as the internal standard.

2.2. Preparation of the Ligands. 2.2.1. Synthesis of L_3. A total of 10 mL of β-phenylethanol and 7 mL of pyridine were mixed, stirred, and heated to 65 °C, then 10 mL of thionyl chloride was added to the mixture. The mixture was stirred and heated at 115 °C under reflux for 1.5 h, after which it was cooled to room temperature, and the white solid appeared. The water was added to the stirring mixture. The organic phase was separated directly from the reaction mixture with a separating funnel. The combined organic phases were dried, and the solvent was removed. The phenylethylchlorine was separated by vacuum distillation under the conditions of 142−143 °C and was then added to the mixture of sodium ethoxide and diethyl malonate (water bath at a constant temperature of 60 °C) under reflux for 4 h. The phenylethyldiethyl malonate was obtained by vacuum distillation under conditions of 172−174 °C and then was hydrolyzed. After about 30 min, the white solid was obtained and extracted and recrystallized. L_3 was obtained with 42.7% yield. ^1H NMR (300 MHz, DMSO-*d*6, dppm): 2.01 (m, 2H, H2), 2.59 (m, 2H, H1), 3.46 (t, 1H, CH_2CH_2CHPh), 7.22 (bm, 5H, Ph).

2.2.2. Synthesis of L_4. L_4 was synthesized in an identical manner to that described for L_3 with β-phenylpropanol in place of β-phenylethanol (32.4% yields). ^1H NMR (300 MHz, DMSO-*d*6, dppm): 1.53 (m, 2H, H3), 1.76 (m, 2H, H2), 2.52 (m, 2H, H1), 2.66 (t, 1H, $CH_2CH_2CH_2CHPh$), 7.18 (bm, 5H, *Ph*).

2.3. Preparation of the Complexes. 2.3.1. Synthesis of the $[Pd(L_1)(bipy)]\cdot 2.5H_2O$ (1). The complex was prepared as follows. A total of 1 mmol of K_2PdCl_4 (0.3264 g) and 1 mmol of phenylmalonate (0.1802 g) were dissolved in 20 mL of water. An ethanol solution (5 mL) containing 1 mmol of 2,2′-bipyridine (0.1562 g) was added dropwise into the mixture. The pH was adjusted to 5.36 by KOH (0.5 M). The solution was stirred for 12 h and filtered. After slow evaporation at room temperature, rectangular crystals were obtained and washed with distilled water. Yield: 57%. Anal. Calcd (%) for $C_{19}H_{19}N_2O_{6.5}Pd$ (**1**): C, 46.98; H, 3.94; N, 5.77. Found (%): C, 46.79; H, 3.89; N, 5.71. IR (KBr): ν_{max}/cm^{-1}: 3109 (m), 3049 (m), 1867 (w), 1605 (s), 1449 (s), 1468 (s), 1165 (m), 1038 (m), 766 (s), 720 (m), 649 (w), 454 (w). ^1H NMR (300 MHz, DMSO-*d*6, dppm): 4.54 (s, 1H, CH*Ph*), 7.80 (d, 2H, H_d, $H_{d'}$), 8.22 (bm, 5H, *Ph*), 8.33 (tt, 2H,

(21) Gao, E. J.; Liu, F. C.; Zhu, M. C.; Wang, L.; Huang, Y.; Liu, H. Y.; Ma, S.; Shi, Q. Z.; Wang, N. *Enzym. Inhib Med. Chem.* **2010**, *25*, 1–8.
(22) José, R.; Julia, L.; Laura, S.; Natalia, C.; Consuelo, V.; María, D. V.; Francesc, X. A.; Gregorio, L.; Virtudes, M.; José, P.; Delia, B. *J. Inorg. Chem.* **2006**, *45*, 6347–6360.
(23) Gao, E. J.; Wang, L.; Zhu, M. C.; Liu, L.; Zhang, W, Z. *Eur. J. Med. Chem.* **2010**, *45*, 311–316.
(24) Elzbieta, B.; Magdalena, M.; Ingo-Peter, L; Peter, M.; Renata, A. K.; Piotr, P.; Urszula, K.; Marek, R. *J. Inorg. Chem.* **2006**, *45*, 9688–9695.
(25) José, R.; María, D. V.; Natalia, C.; Gregorio, L.; Concepción de, H.; Delia, B.; Virtudes, M.; Laura, V. *J. Inorg. Chem.* **2008**, *47*, 4490–4505.
(26) José, R.; Julia, L.; Consuelo, V.; López, G.; José, M. L.; Miguel, M.; Francesc, X,. A.; Delia, B.; Virtudes, M.; Laguna, A. *J. Inorg. Chem.* **2008**, *47*, 6990–7001.
(27) Guddneppanavar, R.; Choudhury, J. R.; Kheradi, A. R.; Steen, B. D.; Saluta, G.; Kucera, G. L.; Day, C. S.; Bierbach, U. *J. Med. Chem.* **2007**, *50*, 2259–2263.
(28) Baruah, H.; Rector, C. L.; Monnier, S. M.; Bierbach, U. *Biochem. Pharmacol.* **2002**, *64*, 191–200.
(29) Gao, E. J.; Zhu, M. C.; Yin, H. X.; Liu, L.; Wu, Q.; Sun, Y. G. *J. Inorg. Biochem.* **2008**, *102*, 1958–1964.
(30) Farrell, N.; Kelland, L. R.; Roberts, J. D.; Beusichem, M. V. *Cancer Res.* **1992**, *52*, 5065–5072.
(31) Beusichem, M. V.; Farrell, N. *Inorg. Chem.* **1992**, *31*, 634–639.
(32) Gao, E. J.; Sun, Y. G.; Liu, Q. T.; Duan, L. Y. *J. Coord. Chem.* **2006**, *59*(11), 1295–1300.
(33) Sun, Y .Z.; Xu, D. J.; Si, Z. L.; Gao, E. J.; Wang, Y. *J. Shenyang Inst. Chem. Technol.* **1997**, *11*, 183–187.

H_c,$H_{c'}$), 8.54 (tt, 2H, H_b, $H_{b'}$), 9.17 (d, 2H, H_a, $H_{a'}$). $^{13}C\{^1H\}$ NMR ($CDCl_3$): $\delta(SiMe_4)$ 174.032 (C=O); 148.332, 124.291, 138.330, 126.968, 155.894 (Ca, Cb, Cc, Cd, Ce of bipy); 66.480 (C0 of phenylmalonate).

2.3.2. Synthesis of the [Pd(L_3)(bipy)]·2H_2O (3). The complex was prepared by the same method used for the preparation of complex **1** except using phenethylmalonate (0.2082 g) instead of phenylmalonate. Yield: 53%. Anal. Calcd (%) for C_{21} H_{22} N_2 O_6 Pd_1 (**3**): C, 49.96; H, 4.39; N, 5.55; Found (%): C, 49.69; H, 4.21; N, 5.45. IR(KBr): ν_{max}/cm^{-1}: 3418 (m), 3085 (w), 2925 (w), 1608 (s), 1452 (m), 1380 (s), 13 465 (w), 1163 (w), 966 (w), 773 (s), 723 (m), 701 (m), 487 (w). ^1H NMR (300 MHz, DMSO-*d*6, dppm): 2.72 (t, 2H, CH_2CH_2CHPh), 2.14 (m, 2H, CH_2CH_2CHPh), 3.63 (t, 1H, CH_2CH_2CHPh), 7.83 (d, 2H, H_d, $H_{d'}$), 8.26 (bm, 5H, *Ph*), 8.30 (tt, 2H, H_c,$H_{c'}$), 8.46 (tt, 2H, H_b, $H_{b'}$), 9.15 (d, 2H, H_a, $H_{a'}$). $^{13}C\{^1H\}$ NMR ($CDCl_3$): $\delta(SiMe_4)$ 174.925 (C=O); 148.390, 124.291, 142.085, 124.256, 156.019 (Ca, Cb, Cc, Cd, Ce of bipy); 33.687, 32.201, 58.413 (C1, C2, C0 of phenethylmalonate).

2.3.3. Synthesis of the [Pd(L_4)(bipy)]·5H_2O (4). The complex was prepared by the same method used for the preparation of complex **1**, except phenylpropylmalonate (0.2220 g) was used instead of phenylmalonate. Yield: 45%. Anal. Calcd (%) for $C_{22}H_{30}N_2O_9$ Pd (**4**): C, 46.12; H, 5.28; N, 4.89. Found (%): C, 46.21; H, 5.24; N, 4.92. IR(KBr): ν_{max}/cm^{-1}: 3427 (m), 3108 (w), 2921 (w), 1602 (s), 1448 (s), 1373 (m), 1164 (m), 1037 (m), 762 (s), 720 (m), 699 (w), 650 (w). ^1H NMR (300 MHz, DMSO-*d*6, dppm): 1.71 (t, 2H, $CH_2CH_2CH_2CHPh$), 1.34 (m, 2H, $CH_2CH_2CH_2CHPh$), 2.52 (m, 2H, $CH_2CH_2CH_2CHPh$), 3.16 (t, 1H, $CH_2CH_2CH_2CHPh$), 7.18 (bm, 5H, *Ph*), 7.79 (d, 2H, H_d, $H_{d'}$), 8.32 (tt, 2H, H_c, $H_{c'}$), 8.59 (tt, 2H, H_b, $H_{b'}$), 9.17 (d, 2H, H_a, $H_{a'}$).$^{13}C\{^1H\}$ NMR ($CDCl_3$): $\delta(SiMe_4)$ 175.303 (C=O); 148.369, 124.221, 142.065, 125.908, 155.964 (Ca, Cb, Cc, Cd, Ce of bipy); 35.555, 30.368, 29.415, 59.507 (C1, C2, C3, C0 of phenylpropylmalonate).

2.4. X-Ray Structure Determination. Single-crystal X-ray data on **1**, **2**, **3**, and **4** were collected at 293(2) K on a BRUKER SMART 1000 CCD detector with graphite-monochromatized Mo Kα radiation (λ = 0.71073 Å) by using the ω-scan technique. Lorentz polarization and absorption corrections were applied. The structures were solved by direct methods and refined with the full-matrix least-squares technique using the SHELXS-97 and SHELXL-97 programs.[34,35] Anisotropic thermal parameters were assigned to all non-hydrogen atoms. The hydrogen atoms were set in calculated positions and refined as riding atoms with a common fixed isotropic thermal parameter. Analytical expressions of neutral-atom scattering factors were employed, and anomalous dispersion corrections were incorporated.

2.5. Determination of Electronic Absorption Spectra. UV−visible spectra were recorded on a Shimadzu UV-240. Tris−HCl buffer (pH 7.0) and a buffer (10 mM) solution of complexes **1**, **2**, **3**, and **4** were titrated with a concentrated fish sperm DNA (FS-DNA) solution. The absorbance of the solution at 308 nm, 260 nm, and 260 nm was measured initially for complexes **1**, **2**, **3**, and **4** after each addition of FS-DNA.

2.6. Fluorescence Spectra. A fluorescence survey was performed on a Perkin-Elmer LS55 spectrofluorometer. For all fluorescence measurements, the entrance and exit slits were maintained at 10 and 10 nm, respectively. The sample was excited at 526 nm and its emission observed at 602 nm. The buffer used in the binding studies was 50 mM Tris−HCl, pH 7.4, containing 10 mM NaCl. The sample was incubated for 4 h at room temperature (20 °C) before spectral measurements.

For the fluorescence quenching experiment, the FS-DNA was pretreated with ethidium bromide (EtBr) in the ratio [DNA]/[EtBr] = 5 for 2 h at room temperature. The metal complexes were then added to the DNA-EtBr system at varying concentrations (1.25−40 μM), and their effect on the emission intensity was measured. The concentration range was limited by precipitation of the DNA at Pd(II) complexes > 55 μM. Under these conditions, the fluorescence intensity of the respective complexes, FS-DNA and EtBr, was very small and could be ignored. The interaction of the respective complexes with DNA in vitro was studied as described in the literature.[36,37]

A fluorescence Scatchard plot was created to study binding constant determination. Essentially, the method is considered to be the titration of a given amount of DNA−metal complexes with increasing concentrations of EtBr (0.5−5 μM) and measurement of the changes in fluorescence intensity. The binding isotherms were obtained from the Scatchard equation:[38] $r_b/c = K_{app}(n - r_b)$, where r_b is the number of molecules bound per DNA nucleotide phosphate, c is the free drug concentration, and K_{app} is the apparent binding constant. A plot of experimentally determined r_b/c values versus r_b yields a value for n, the maximum number of binding sites per DNA base pair, from the x intercept. r_b can be determined by the equation $r_b = n - r_E - r_E/(K_E \cdot c_E)$,[39] where c_E is the concentration of free ethidium and K_E is a linear Scatchard constant dependent on the ratio of the bound concentration of EtBr to the concentration of DNA, and the K_E value is obtained as the slope of the r_E/C_E versus r_E linear plot.[38] Different DNA−metal complexes correspond to different values of r_f, where r_f is the formal ratio of the complex to nucleotide concentration with values ranging from 0 to 3.5. The plot of r_b/c versus r_b gives the association constant (slope) and the apparent binding site size (x intercept) for the agents.

2.7. Plasmid DNA Cleavage by Complexes. The plasmid DNA, pBR322 (as a solution in Tris buffer), with a length of 436 bp was purchased from Biopolymers, Inc. and kept at −20 °C. The sample was incubated at 310 K for an appropriate time, and a loading buffer was applied (0.25% bromphenol blue, 50% glycerol). The gel electrophoresis experiments were performed by incubation at 310 K for 5 min of 0.5 mg·mL^{-1} pBR322 DNA and a 20 μM metal complex in a loading buffer (0.25% bromphenol blue, 50% glycerol). Concentration of the metal complex was also varied from 20 to 120 μM. After incubation, the solution was then subjected to electrophoresis on 0.8% agarose gel in a TAE buffer (40 mM Tris acetate/1 mMEDTA) at 120 V for 120 min. Gels were stained with ethidium bromide and visualized under a UV transilluminator and photographed using a digital camera. In all cases, the background fluorescence was subtracted. A correction factor of 1.42 was used for supercoiled DNA (form I) assessment since the intercalation between EtBr and form I DNA is relatively weak compared with that of nicked (form II) and linear DNA (form III).[40−43]

2.8. Cell Line and Culture. The cell lines used in this experiment were routinely maintained in a RPMI-1640 medium supplemented with 10% (v/v) heat-inactivated fetal bovine serum, 2 mmol/L of glutamine, 100 U/mL of penicillin, and

(34) Sheldrick, G. M. *SHELXS 97*; University of Gottingen: Gottingen, Germany, 1997.
(35) Sheldrick, G. M. *SHELXL 97*; University of Gottingen: Gottingen, Germany, 1997.
(36) Mital, R.; Srivastava, T. S. *J. Inorg. Biochem.* **1990**, *40*, 111–120.
(37) vital, R.; Srivastava, T. S.; Parekh, H. K.; Chitnis, M. P. *J. Inorg. Biochem.* **1991**, *41*, 93–103.
(38) Scatchard, G.; Ann., N. Y. *Acad. Sci.* **1949**, *51*, 660–672.
(39) Howe-Grant, M; Wu, K. C.; Bauer, W. R; Lippard., S. J. *Biochemistry* **1976**, *15*, 4339.
(40) Dhar, S.; Reddy, P. A. N.; Chakravarty, A. R. *Dalton Trans.* **2004**, 697–698.
(41) Sreedhara, A.; Freed, J. D.; Cowan, J. A. *J. Am. Chem. Soc.* **2000**, *122*, 8814–8824.
(42) Brannum, M.; Tipton, A. K.; Zhu, S.; Que, L. J. *J. Am. Chem. Soc.* **2001**, *123*, 1898–1904.
(43) Itoh, U.; Hisada, H.; Sumiya, T.; Hosono, M.; Sui, Y. U.; Fu Ji, Y. *Chem.Commun.* **1997**, 677–678.

Table 1. Crywstallographic Data for **1**, **3**, and **4**

	1	3	4
formula	$C_{152}H_{152}N_{16}O_{52}Pd_8$	$C_{42}H_{44}N_4O_{12}Pd_2$	$C_{44}H_{60}N_4O_{18}Pd_2$
fw	3886.31	1009.61	4498.59
cryst syst	monoclinic	tetragonal	monoclinic
space group	$C\,1\,2/c\,1$	$I\,\bar{4}\,2\,d$	$P\,1\,21/c\,1$
a (Å)	18.618(4)	28.800(4)	11.1538(10)
b (Å)	12.933(5)	28.800(4)	19.7003(17)
c (Å)	16.650(3)	10.802(3)	22.4414(19)
α (deg)	90	90	90
β (deg)	110.31(3)	90	90.46(0)
γ (deg)	90	90	90
V (Å^3)	3759.8(18)	8959(3)	4930.96(74)
Z	1	8	4
Dc (g cm^{-3})	1.716	1.497	1.542
μ (mm^{-1})	1.030	0.866	0.805
reflns collected	11300	25293	26156
unique reflns	3316	4600	9366
GOF	1.098	1.075	1.154
R_1 ($I > 2\sigma(I)$)[a]	0.0585	0.0647	0.0731
wR_2 (all data)[b]	0.1283	0.1644	0.1965
ΔFmax (e ·Å^{-3})	1.744	0.622	1.975
ΔFmin (e ·Å^{-3})	−0.975	−0.348	−0.708

[a] $R_1 = \Sigma||F_o| - |F_c||/\sum|F_o|$, $wR_2 = [\Sigma[w(F_o^2 - F_c^2)^2]/\Sigma w(F_o^2)^2]^{0.5}$. [b] $w = 1/[\sigma^2(F_o^2) + (aP)^2 + bP]$, where $P = (2F_c^2 + F_o^2)/3$ and a and b are constants set by the program.

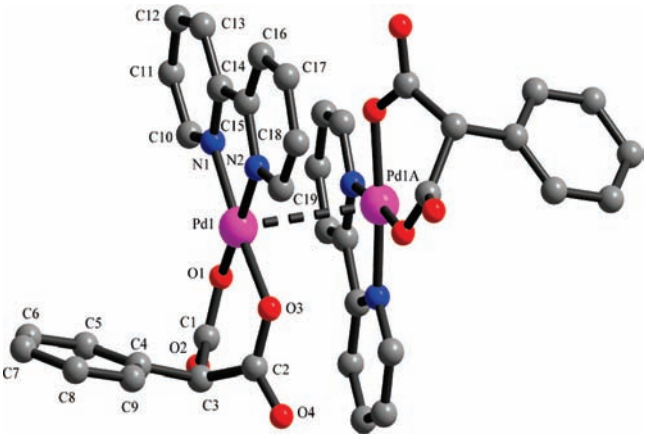

Figure 1. ORTEP representation (50% probability) of **1**. Selected bond lengths (Å) and angles (deg): Pd1−N1 = 1.987(3), Pd(1)−N(2) = 1.992(3), Pd(1)−O(1) = 1.981(3), Pd(1)−O(3) = 1.995(3), N(1)−Pd(1)−N(2) = 81.24(13), O(1)−Pd(1)−O(3) = 92.23(11).

100 μg/mL of streptomycin in a highly humidified atmosphere of 95% air with 5% CO_2 at 37 °C.

2.9. Cell Sensitivity Assay. The growth inhibitory effect of metal complexes on the HeLa cells, the Hep-G2 cells, the KB cells, and the AGZY-83a cells was measured using the microculture tetrazolium [3-(4,5-dimethylthiazol-2-yl)-2,5-diphenyltetrazolium bromide, MTT] assay.[44] In brief, cells were seeded into a 96-well culture plate at 2×10^5 cells/well in a 100 μL culture medium. After incubation for 24 h, cells were exposed to the tested complexes of serial concentrations. The complexes were dissolved in DMF and diluted with RPMI 1640 or DMEM to the required concentrations prior to use (0.1% DMF final concentration). The cells were incubated for 24 h and 72 h, followed by the addition of a 20 μL MTT solution (5 mg/mL) to each well and further cultivation for 4 h. The media with MTT were removed, and 100 μL of DMSO was added to dissolve the

(44) Alley, M. C.; Scudiero, D. A.; Monks, A.; Hursey, M. L.; Czerwinski, M. J.; Fine, D. L.; Abbott, B. J.; Mayo, J. G.; Shoemaker, R. H.; Boyd, M. R. *Cancer Res.* **1988**, *48*, 589–601.

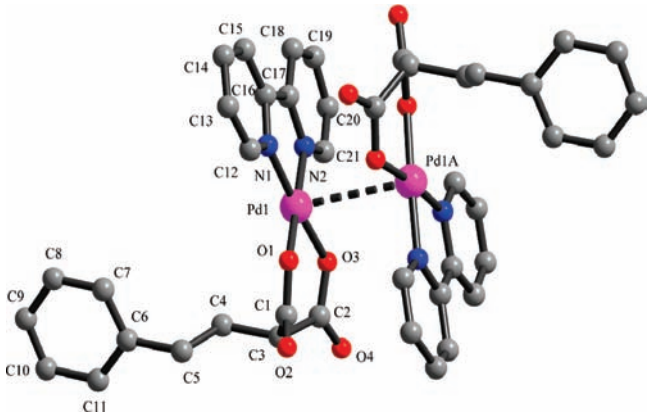

Figure 2. ORTEP representation (50% probability) of **3**. Selected bond lengths (Å) and angles (deg): Pd(1)−N(1) = 1.961(10), Pd(1)−N(2) = 1.979(9), Pd(1)−O(1) = 1.997(6), Pd(1)−O(3) = 1.988(8), N(1)−Pd(1)−N(2) = 81.6(4), O(3)−Pd(1)−O(1) = 93.2(3).

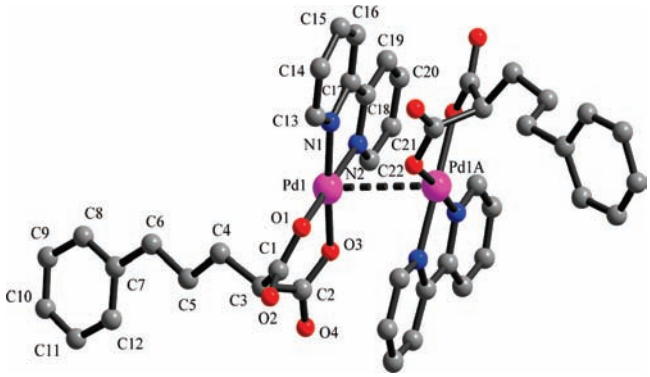

Figure 3. ORTEP representation (50% probability) of **4**. Selected bond lengths (Å) and angles (deg): Pd(1)−N(3) = 1.996(6), Pd(1)−N(4) = 2.001(6), Pd(1)−O(6) = 1.989(5), Pd(1)−O(8) = 2.014(5), N(3)−Pd(1)−N(4) = 81.6(2), O(6)−Pd(1)−O(8) = 92.1(2)).

formazan crystals at room temperature for 30 min. The absorbance of each cell at 450 nm was determined by analysis with a microplate spectrophotometer. The IC_{50} values were obtained from the results of quadruplicate determinations of at least three independent experiments.

In another experiment, the effect on cell growth for the two complexes and cisplatin was studied by culturing the cells in medium alone for 24 h, followed by 48 h treatment with 5 μM concentrations. The viable cells remaining at the end of the treatment period were determined by MTT assay and calculated as the percent of control, treated with the vehicle alone (DMSO) under similar conditions.

2.10. In Vitro Apoptosis Assay. The in vitro induction of apoptosis by the metal complexes **1**−**4** was determined by a flow cytometry assay with Annexin V-FITC29by using an Annexin V-FITC Apoptosis Detection Kit (Roche). Exponentially growing HeLa cells, Hep-G2 cells, KB cells, and AGZY-83a cells in 6-well plates (6×10^5 cells/well) were exposed to concentrations equal to the IC_{50} of the cisplatin or complexes **1**−**4** for 24 h. After the cells were subjected to staining with the Annexin V-FITC and propidium iodide, the amount of apoptotic cells was analyzed by flow cytometry (BD FACSCalibur).

2.11. Structures of the Four Complexes. The single-crystal X-ray analysis reveals that complexes **1**, **2**, **3**, and **4** are similar in structure, while the structure of complex **2** was reported previously by ourselves.[32] The difference in the complexes will be discussed in relative to complex **1**. A summary of data collection and refinement for the three complexes is presented in Table 1.

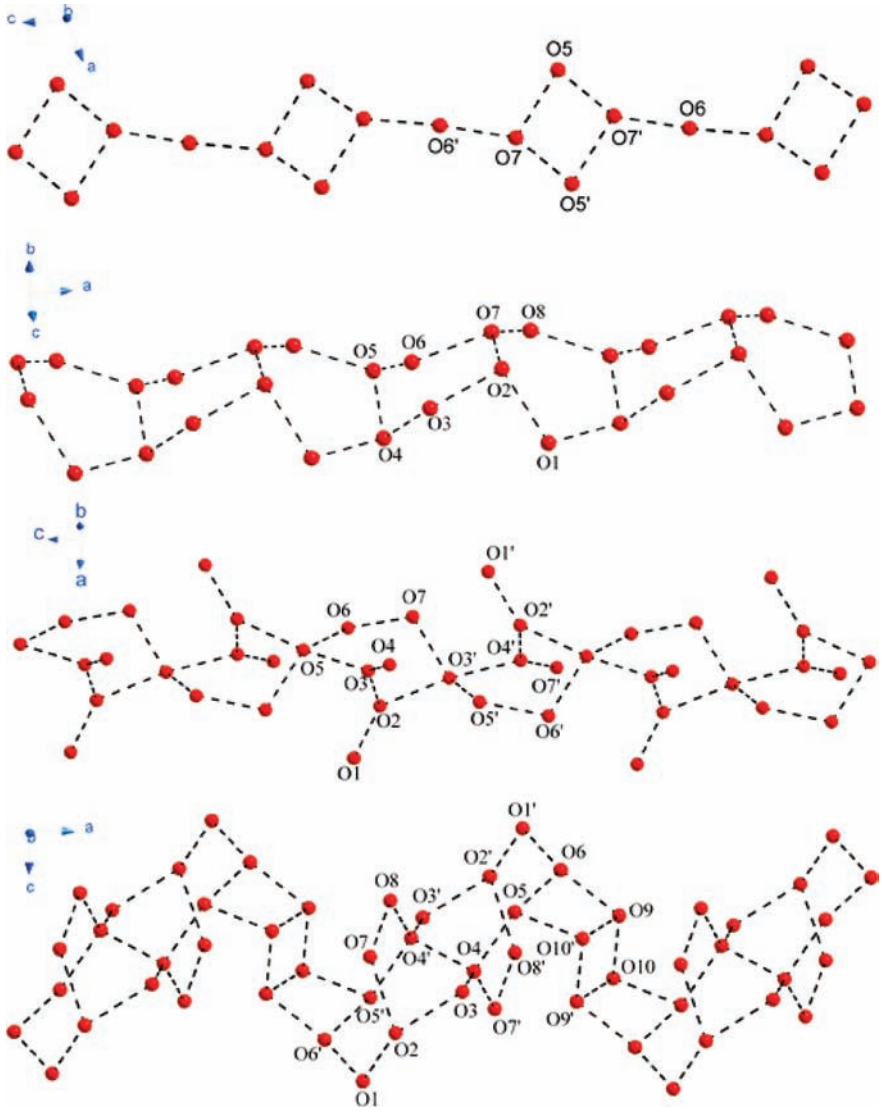

Figure 4. The 1D water cluster in four complexes formed by a unit of $(H_2O)_5$ in **1**, $(H_2O)_8$ in **2**, $(H_2O)_{14}$ in **3**, and $(H_2O)_{20}$ in **4**.

Figures 1−3 show the thermal ellipsoid perspectives for complexes **1**, **3**, and **4**, respectively.

3. Results and Discussion

3.1. Structure of the Four Complexes. The geometry around Pd(II) of the four complexes is approximately square planar, composed of two nitrogen atoms from the bipyridine and two oxygen atoms from phenylalkylmalonic acid, showing similar local coordination environments. The fundamental unit of complex **1** consists of two homologous isomers. Each isomer has one palladium(II), one bipy ligand, and one L_1 ligand, as shown in Figure 1. The palladium(II) is coordinated with two N atoms (Pd1−N1 = 1.987(3), Pd(1)−N(2) = 1.992(3)) from one bipy and two oxygen atoms (Pd(1)−O(1) = 1.981(3), Pd(1)−O(3) = 1.995(3)) from phenylmalonic acid (complex **2**: Pd(1)−N(1) = 1.992(7), Pd(1)−N(2) = 1.997(6), Pd(1)−O(1) = 1.986(5), Pd(1)−O(3) = 1.997(6); complex **3**: Pd(1)−N(1) = 1.961(10), Pd(1)−N(2) = 1.979(9), Pd(1)−O(1) = 1.997(6), Pd(1)−O(3) = 1.988(8); complex **4**: Pd(1)−N(3) = 1.996(6), Pd(1)−N(4) = 2.001(6), Pd(1)−O(6) = 1.989(5), Pd(1)−O(8) = 2.014(5)). The distances compare well with those found in the literature for palladium complexes.[45−49] Intermolecular benzene−bipy CH···π interactions[50] are found and are also responsible for the formation of extensive networks of **1** and **2** with distance of 3.267 Å and 3.137 Å, respectively. However, $\pi\cdots\pi$ stacking is found to construct the supermolecular structures of **3** and **4** with distances of 3.813 Å and 3.710 Å (centroid−centroid). The distance of adjacent Pd···Pd is 3.187(10) Å in **1**, 3.902(14) Å in **2**, 3.205(15) Å in **3**, and 3.357(12) Å in **4**, which is larger than the range of known Pd···Pd lengths (2.391−3.185 Å) presenting weak attractive metal−metal interactions.[51,52]

(45) Ruiz, J.; Cutillas, N.; Vicente, C.; Villa, M. D.; López, G.; Lorenzo, J.; Avilés, F. X.; Moreno, V.; Bautista, D. *Inorg. Chem.* **2005**, *44*, 7365–7376.
(46) Lakomska, I.; Szlyk, E.; Sitkowski, J.; Kozerski, L.; Wietrzyk, J.; Pelczynska, M.; Nasulewicz, A.; Opolski, A. *J. Inorg. Biochem.* **2004**, *98*, 167–172.
(47) Szlyk, E.; Grodzicki, A.; Pazderski, L.; Wojtczak, A.; Chatlas, J.; Wrzeszcz, G.; Sitkowski, J.; Kamienski, B. *J. Chem. Soc., Dalton Trans.* **2000**, 867–872.
(48) Szlyk, E.; Lakomska, I.; Surdykowski, A.; Glowiak, T.; Pazderski, L.; Sitkowski, J.; Kozerski, L. *Inorg. Chim. Acta* **2002**, *333*, 93–99.
(49) Szlyk, E.; Pazderski, L.; Lakomska, I.; Surdykowski, A.; Glowiak, T.; Sitkowski, J.; Kozerski, L. *Polyhedron* **2002**, *21*, 343–348.
(50) Nishio, M. *CrystEngComm* **2004**, *6*, 130–158.

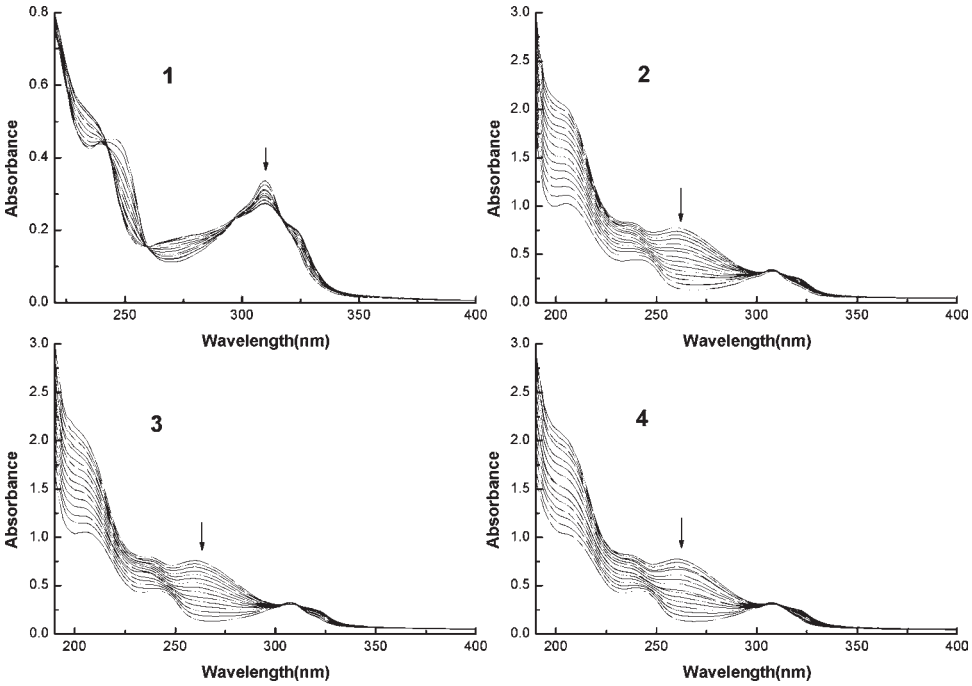

Figure 5. Effect of FS-DNA on the absorption spectrum of complexes: (1) complex **1** (20 μM), (2) complex **2** (20 μM), (3) complex **3** (20 μM), (4) complex **4** (20 μM). The DNA concentration increase on the order of 0−48 μM. The arrow shows the absorbance changes upon increasing the DNA concentration.

The crystallization water molecules, playing an important role in defining the supramolecular structure of the four complexes, are interconnected by hydrogen bonds to build an ordered 1D water chain. An interesting feature is that the 1D water cluster becomes larger as the length chain grows longer (Figure 4). As indicated by analysis, the $(H_2O)_5$ water cluster of **1** consists of one water tetramer and one water monomer. Each water tetramer (O5, O7 and symmetry atom) is bridged by one water monomer (O6) to assemble a 1D water cluster. In **2**, the $(H_2O)_8$ water cluster is formed by four uncoordinated waters with one hexagon (O2, O3, O4, O5, O6, O7) and two water monomers (O1, O8). Each hexagon is connected to a corrugated sheet by the two monomers. In **3**, the $(H_2O)_{14}$ water is formed by four uncoordinated water clusters. Each water cluster consisted of a cyclic 12-member ring (O1, O2, O3, O4, O5, O6, and O7 and their symmetrical atoms) with two knobs (O7, O8 and O7′, O8′) and one rectangle (O9, O10, O9′, O10′). The 12-member rings assembled a 1D water cluster by the rectangles. In **3**, the $(H_2O)_{20}$ water cluster is formed by 10 uncoordinated water molecules. The infinite 1D chains of $(H_2O)_{20}$ clusters each consist of two basic cyclic six-member rings (O1, O3, O4, O4, O5 and O6) each fused with a four-member structure (O7, O8, O9 and O10) and one water monomer (O2), which is in between a six-member ring and four-member ring. The average O···O distances of complexes **1** and **3** (2.693 Å and 2.697 Å) are lower than the corresponding value of 2.745 Å reported in ref 53 and larger than the value of 2.629 Å reported in ref 54. However, the average O···O distances of complexes **2** and **4** (2.777 Å and 2.797 Å) are larger than the values reported in ref 54.

3.2. DNA Binding. Electronic absorption spectroscopy is an effective method to examine the binding mode of DNA with metal complexes.[53] If the binding mode is intercalation, the π^* orbital of the intercalated ligand can couple with the π orbital of the DNA base pairs, thus, decreasing the $\pi-\pi^*$ transition energy and resulting in bathochromism. On the other hand, the coupling π orbital is partially filled by electrons, thus, decreasing the transition probabilities and concomitantly resulting in hypochromism.[54] It is a general observation that the binding of an intercalative molecule to DNA is accompanied by hypochromism and a significant red-shift (bathochromism) in the absorption spectra due to a strong stacking interaction between the aromatic chromophore of the ligand and DNA base pairs with the extent of hypochromism and a red-shift commonly consistent with the strength of intercalative interaction.[53] Thus, in order to provide evidence for the possibility of binding of each complex to FS-DNA, spectroscopic titration of a solution of the complexes with FS-DNA has been performed.[55] As shown in Figure 5, the potential FS-DNA binding ability of complexes was studied by UV spectroscopy by following the intensity changes of the intraligand $\pi-\pi^*$ transition band at 244, 253, 260, 265 nm. Upon the addition of an increasing amount of FS-DNA to the complexes, the hypochromism and a slight red-shift were observed, which indicates moderate binding of the complexes with DNA. A similar hypochromism was previously observed for other complexes.[56] The spectral changes

(51) Novoa, J. J.; Aullón, G.; Alemany, P.; Alvarez, S. *J. Am. Chem. Soc.* **1995**, *117*, 7169–7171.
(52) Aullón, G.; Alemany, P.; Alvarez, S. *Inorg. Chem.* **1996**, *35*, 5061–5067.
(53) Kelly, T. M.; Tossi, A. B.; McConnell, D. J.; Strekas, T. C. *Nucleic Acids Res.* **1985**, *13*, 6017–6034.
(54) Pyle, A. M.; Rehmann, J. P.; Meshoyrer, R.; Kumar, C. V.; Turro, N. J.; Barton, J. K. *J. Am. Chem. Soc.* **1989**, *111*, 3053–3063.
(55) Chao, H.; Mei, W. J.; Huang, Q. W.; Ji, L. N. *J. Inorg. Biochem.* **2002**, *92*, 165–170.

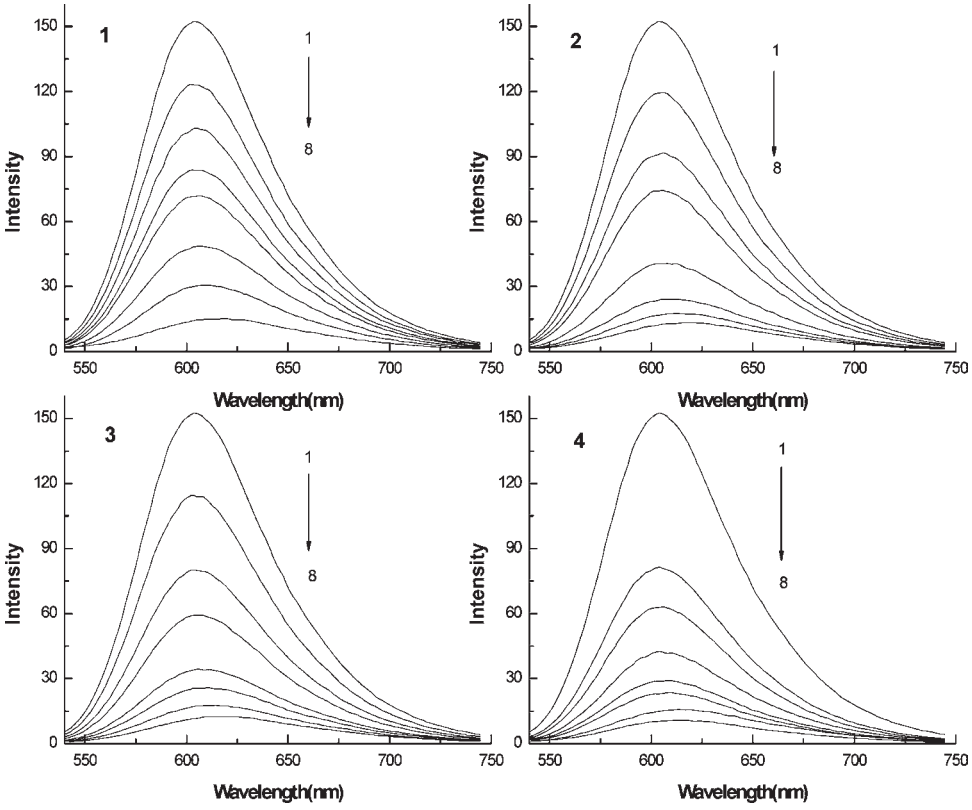

Figure 6. Fluorescence spectra of the binding of EtBr to DNA in the absence (line 1) and presence (line 2) of increasing amounts of the complexes λ_{ex} = 526 nm, C_{EtBr} = 1.0 μM, C_{DNA} = 5.1 μM, $C_{M(1-4)}$ (line 2−8): 1.25, 2.5, 3.75, 6.25, 10, 25, 40 (μM).

are characterized by one or more isosbestic points (complex **1**: 240 nm, 260 nm, 294 nm, 316 nm; complex **2**: 308 nm; complex **3**: 307 nm, 313 nm; complex **4**: 307 nm, 313 nm) well maintained until the end of the titrations of the complexes with DNA so one can rule out the presence of species other than the free and the intercalated complexes. The presence of these isosbestic points indicates that there is equilibrium between bound DNA and the free form of the metal complexes.[57−59]

Fluorescence quenching measurements can be used to monitor metal binding.[60] The emission intensity of ethidium bromide (EtBr) is used as a spectral probe. EtBr shows reduced emission intensity ina buffer because of quenching by solvent molecules and a significant enhancement of the intensity when bound to DNA. Binding of the complexes to DNA decreases the emission intensity, and the extent of the reduction of the emission intensity gives a measure of the DNA binding propensity of the complexes and stacking interaction (intercalation) between the adjacent DNA base pairs.

According to the classical Stern−Volmer equation,[61] $I_0/I = 1 + K_{sq}r$, where I_0 and I represent the fluorescence intensities in the absence and presence of the complex, respectively, and r is the concentration ratio of the complex to DNA. K_{sq} is a linear Stern−Volmer quenching constant dependent on the ratio of the bound concentration of EtBr to the concentration of DNA. The K_{sq} value is obtained as the slope of an I_0/I versus r linear plot. The fluorescence-quenching curve of DNA-bound EtBr by the four complexes is given in Figure 6. As shown in Figure 7, the quenching curves illustrate that the complexes bind to DNA in the series of K_{sq} **4** > K_{sq} **3** > K_{sq} **2** > K_{sq} **1**. The data indicate that the four complexes bound to DNA with different binding affinities, in the order complex **4** > complex **3** > complex **2** > complex **1**, which

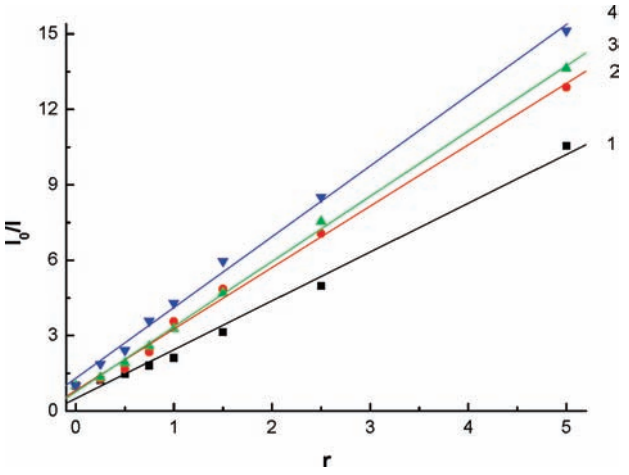

Figure 7. Stern−Volmer quenching plots of the complexes **1**, **2**, **3**, and **4** with the value of slope being 1.94 (complex **1**), 2.44 (complex **2**), 2.59 (complex **3**), and 2.81 (complex **4**).

(56) Milani, B.; Marson, A.; Zangrando, E.; Mestroni, G.; Ernsting, J. M. *Inorg. Chim. Acta* **2002**, *188*, 327–331.
(57) Torshizi, H. M.; Srivastava, T. S.; Chavan, S. J.; Chitnis, M. P. *J. Inorg. Biochem.* **1992**, *48*, 1163–1170.
(58) Blake, A; Peacoke, A. R. *Biopolymers* **1967**, *6*, 87–92.
(59) Paul, A. K.; Srivastava, T. S.; Chavan, S. J.; Chitnis, M. P.; Desai, S.; Rao, K. K. *J. Inorg. Biochem.* **1996**, *61*, 179–196.
(60) Yang, B. S.; Feng, J. Y.; Li, Y. Q.; Gao, F.; Zhao, Y. Q.; Wang, J. L. *J. Inorg. Biochem.* **2003**, *96*, 416–424.
(61) Lakowicz, J. R.; Weber, G. *Biochemistry* **1973**, *12*, 4161–4170.

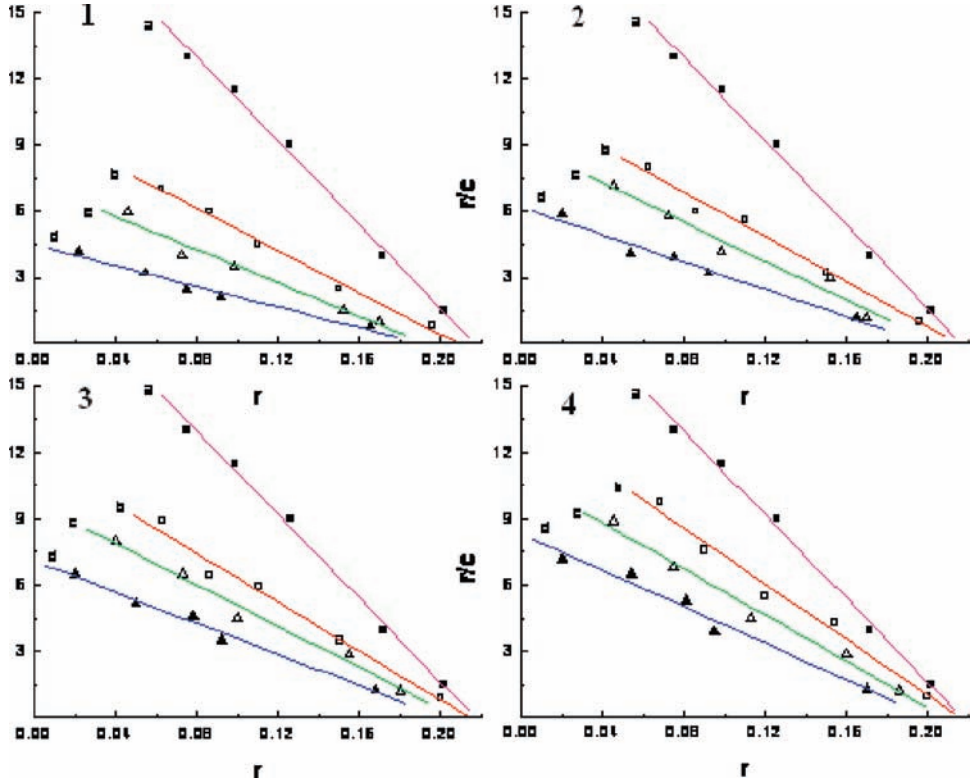

Figure 8. Fluorescence Scatchard plots for the binding of EtBr (0.5−5 M) to DNA in the absence (line a) and the presence (lines b−d) of increasing concentrations of complexes **1**, **2**, **3**, and **4**. r_f increases in the range of 0.102 to 2.116 for the four complexes.

Table 2. Binding Parameters for Fluorescence Scatchard Plot of Calf Thymus DNA with EB in the Presence of Complexes **1**, **2**, **3**, and **4**.

complex	r_f	K_{obs} ($\times 10^5$ M^{-1})	n
1	0.000	9.4622	0.2169
	0.104 ± 0.003	4.7571 ± 0.0009	0.2083 ± 0.0008
	1.071 ± 0.005	3.7856 ± 0.0011	0.1922 ± 0.0018
	2.116 ± 0.006	2.3316 ± 0.0013	0.1913 ± 0.0013
2	0.000	9.4622	0.2169
	0.109 ± 0.012	5.0686 ± 0.0019	0.2148 ± 0.0021
	1.023 ± 0.009	4.3792 ± 0.0014	0.2055 ± 0.0017
	2.065 ± 0.017	3.1017 ± 0.0023	0.1992 ± 0.0025
3	0.000	9.4622	0.2169
	0.102 ± 0.003	5.5274 ± 0.0007	0.2143 ± 0.0014
	1.050 ± 0.013	4.6773 ± 0.0021	0.2084 ± 0.0013
	2.140 ± 0.011	3.5222 ± 0.0018	0.2012 ± 0.0027
4	0.000	9.4622	0.2169
	0.096 ± 0.015	6.3155 ± 0.0017	0.2157 ± 0.0016
	1.009 ± 0.017	5.2167 ± 0.0028	0.2090 ± 0.0029
	2.098 ± 0.024	4.1287 ± 0.0032	0.2012 ± 0.0027

indicates that the ability of binding to DNA increases gradually as the length of aliphatic chain becomes longer.

The fluorescence Scatchard plot is an important tool to determine how the complex binds to FS-DNA, which can provide the binding mode of the complexes to DNA.[62] The fluorescence Scatchard plots obtained for competition of the complexes with EtBr to bind with DNA are given in Figure 8. The binding parameters for fluorescence scatchard plots of FS-DNA with EtBr in the presence of complexes are shown in Table 2. The apparent binding constant (K_{app}) values are calculated, and the values are 0.64×10^7 M^{-1} (**1**), 1.07×10^7 M^{-1} (**2**), 1.6×10^7 M^{-1} (**3**), and 3.2×10^7 M^{-1} (**4**), respectively, which

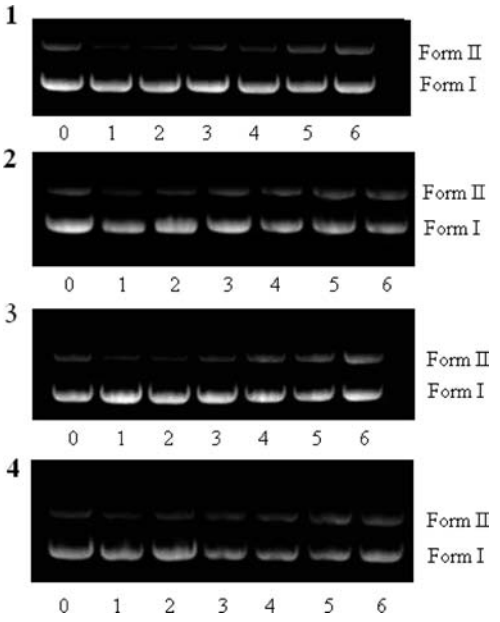

Figure 9. Cleavage of pBR322 DNA(10 μM) in the presence of Pd(II) complexes, lane 0, DNA alone. Lanes 1−6 at different concentrations of the complexes: (1) 20, (2) 40, (3) 60, (4) 80, (5) 100, (6) 120 μM (1, complex **1**; (2) complex **3**; (3) complex **3**; (4) complex **4**).

also displays a similar affinity and binding site size with EtBr (the binding constants of the classical intercalators and metallointercalators were on the order of 10^7 M^{-1}).[63] The result (n = 0.22) suggests that the interaction of the

(62) Howe-Grant, M.; Wu, K. C.; Bauer, W. R.; Lippard, S. J. *Biochemistry* **1976**, *15*, 4339–4346.

(63) Cory, M.; Mckee, D. D.; Kagan, J.; Henryand, D. W.; Miller, J. A. *J. Am. Chem. Soc.* **1985**, *107*, 2528–2530.

Table 3. Cytotoxicity of the Complexes and Cisplatin against Selected Human Tumor Cells after 24 h and 72 h of Incubation (Data Are Expressed as Mean ± SD (n = 4))

		in vitro activity (IC_{50} ± SD, μM)				
time of incubation	tumor cells	complex **1**	complex **2**	complex **3**	complex **4**	cisplatin
24 h	Hela	21.67 ± 4.36	18.05 ± 3.21	15.39 ± 2.87	9.64 ± 1.98	16.54 ± 3.13
	Hep-G2	15.97 ± 2.52	12.84 ± 2.34	6.38 ± 1.67	3.23 ± 0.68	6.93 ± 1.89
	KB	31.27 ± 7.38	26.39 ± 5.47	22.15 ± 4.13	15.82 ± 2.86	10.57 ± 1.62
	AGZY-83a	47.17 ± 7.68	39.65 ± 6.94	32.54 ± 5.73	20.47 ± 4.32	11.82 ± 3.27
72 h	Hela	6.58 ± 1.94	4.62 ± 0.95	2.36 ± 0.41	1.13 ± 0.22	0.84 ± 0.16
	Hep-G2	5.71 ± 1.24	3.64 ± 0.71	1.83 ± 0.32	1.23 ± 0.24	1.83 ± 0.38
	KB	9.23 ± 1.73	7.95 ± 1.67	5.69 ± 1.18	3.57 ± 0.53	1.64 ± 0.31
	AGZY-83a	11.28 ± 3.24	9.31 ± 1.67	6.92 ± 1.34	4.65 ± 0.91	2.29 ± 0.54

four complexes with DNA is in the strong intercalative mode. The length of the aliphatic chain becomes longer, resulting in an increase of the K_{app} value of the four complexes, which is also in agreement with the above proposal.

3.3. DNA Cleavage by the Four Complexes. The cleavage of pBR322 DNA in the absence and presence of Pd(II) complexes was carried out in a 50 mM Tris−HCl buffer (pH 8.0), 18 mM NaCl under UV irradiation. The activities of **1**, **2**, **3**, and **4** were assessed by the conversion of DNA from form I to form II or form III. As shown in Figure 9, with the increase of the complex concentration, the intensity of the circular supercoiled DNA (form I) band decreases, while that of the nicked (form II) band apparently increases (lanes 1−6). The complexes can cleave the supercoiled DNA to nicked circular DNA under aerobic conditions, illustrating the cleavage of plasmid pBR322 DNA induced by the four complexes at different concentrations, respectively. Moreover, complex **4** exhibits more effective DNA cleavage activity than other complexes at the same concentration. Furthermore, enhanced activity was found under physiological conditions. The strong interaction with DNA is not unusual for this class of palladium(II) complexes, and it has a number of structural similarities to many known for palladium-(II), including those that are known to thread their way through the DNA double helix.[64]

3.4. Cytotoxicity Assays. The in vitro growth inhibitory effect of the new complexes **1**−**4** and cisplatin was evaluated in the HeLa cells, the Hep-G2 cells, the KB cells, and the AGZY-83a cells. The IC_{50} values of the four complexes are listed in Table 3. In addition, Figure 10 reveals the effect on cell growth after a treatment period of 48 h with a 5 μM concentration.

Among the complexes studied here, complex **4** is found to be the most active against the cancer cells tested, while complex **1** is the least active. The complexes all have higher cytotoxic activity against the Hep-G2 cell line than others cell lines used. A viability rate by day 3 to less than 50% of the control values was observed for the complexes. The complexes were more effective in arresting the growth of Hep-G2 than other lines. The results coincide with IC_{50} values. As evaluated by the results, the cytotoxicity of the complexes has an apparent dependence on the length of the aliphatic chain increases. The relationship between the length of the linking hydrocarbon chain and the inhibitory ability has been also studied by

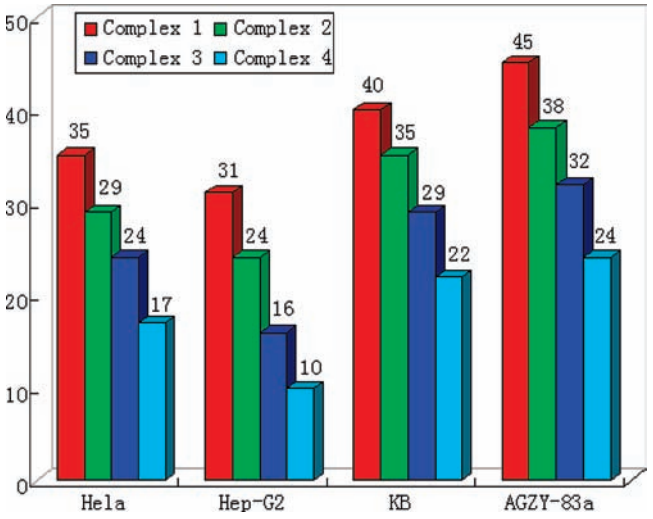

Figure 10. Effect of 5 μg/mL of the complexes on breast cancer cells' viability. All determinations are expressed as a percentage of the control (untreated cells).

Kalayda and his co-worker.[65] This trend may be due to the greater lipophilicities of the higher analogues, although changes in DNA binding mode across the series could also play a role.[66]

3.5. In Vitro Apoptosis Assay. The most common and well-defined form of programmed cell death is apoptosis, which is a physiological cell suicide program that is essential for the maintenance of tissue homeostasis in multicellular organisms. In contrast to the self-contained nature of apoptotic cell death, necrosis is a messy, unregulated process of traumatic cell destruction, which is followed by the release of intracellular components.[67] In order to observe in which way the new complexes produced the cellular death (necrosis or apoptosis), studies of flow cytometry[68−72] were performed on the HeLa cells, the Hep-G2 cells, the KB cells, and the AGZY-83a cells. The complexes were incubated for 24 h at a concentration close to the IC_{50}. With all complexes, apoptosis was observed, and the percentages are presented in Table 4. This assay showed that the studied complexes, in general, induced apoptosis and produced the death of the larger

(64) Onfelt, B.; Lincoln, P.; Norden, B. *J. Am. Chem. Soc.* **2001**, *123*, 3630–3637.
(65) Kalayda, G. V.; Zhang, G.; Abraham, T.; Tanke, H. J; Reedijk, J. *J. Med. Chem.* **2005**, *48*, 5191–5202.
(66) Tysoe, S. A.; Morgan, R. J.; Baker, A. D.; Strekas, T. C. *J. Phys. Chem.* **1993**, *97*, 1707–1713.
(67) Martin, S. J.; Green, D. R. *Curr. Opin. Oncol.* **1994**, *6*, 616–621.
(68) Darzynkiewicz, Z.; Bruno, S.; Del Bino, G.; Gorczyca, W.; Hotz, M. A.; Lassota, P.; Traganos, F. *Cytometry*. **1992**, *13*, 795–808.
(69) Vaux, D. L. *Proc. Natl. Acad. Sci. U. S. A.* **1993**, *90*, 786–789.
(70) Bursch, W. *Biochem. Cell Biol.* **1990**, *68*, 1071–1074.
(71) Williams, G. T. *Cell* **1991**, *65*, 1097–1098.
(72) Cotter, T. G. *Anticancer Res.* **1990**, *10*, 1153–1160.

Table 4. Percentages of Vital Cells, Apoptotic Cells, Dead Cells, and Damaged Cells after Treatment of the Cells Population with Cisplatin and Complexes **1**−**4** for 24 h

cells	treatment (IC_{50} 24 h, μM)	vital cells (%)	apoptotic cells (%)	late apoptotic and/or late necrotic cells (%)	necrotic cells (%)
Hela	control	87.93	5.86	5.38	0.83
	complex **1** (21.67)	47.24	41.37	10.56	0.83
	complex **2** (18.05)	49.47	40.33	9.28	0.92
	complex **3** (15.39)	54.39	39.64	4.96	1.01
	complex **4** (9.64)	58.63	35.78	4.78	0.82
	cisplatin (16.54)	52.73	41.86	4.62	0.79
Hep-G2	control	89.96	4.32	4.88	0.84
	complex **1** (15.97)	56.49	31.24	11.35	0.92
	complex **2** (12.84)	58.37	30.35	10.32	0.76
	complex **3** (6.54)	64.57	25.39	9.15	0.89
	complex **4** (2.71)	69.31	21.73	7.93	1.04
	cisplatin (6.93)	61.84	32.17	4.64	1.36
KB	control	88.07	6.73	4.49	0.71
	complex **1** (31.27)	57.39	32.57	9.22	0.82
	complex **2** (26.39)	61.74	25.42	11.87	0.97
	complex **3** (22.15)	66.83	24.52	7.96	0.69
	complex **4** (15.82)	69.41	20.27	9.55	0.78
	cisplatin (10.57)	75.68	12.76	10.54	1.02
AGZY-83a	control	87.24	8.03	4.23	0.45
	complex **1** (47.17)	48.85	35.67	14.83	0.65
	complex **2** (39.65)	51.39	33.27	14.09	1.24
	complex **3** (32.54)	54.96	32.38	11.68	0.98
	complex **4** (20.47)	59.49	30.52	9.12	0.87
	cisplatin (11.82)	62.38	26.47	10.24	0.91

amount of cells by this pathway. In general, low percentages of cell death by necrosis were obtained.

4. Conclusions

The series of organometallic Pd(II) complexes with a benzenealkyl dicarboxlate chain has been prepared, showing the impact of the length of carbon chain on the structures. The DNA-binding properties of the complexes were examined by the UV−visible spectra and fluorescence spectra, which suggest their involvement in intercalative DNA interaction with different binding affinities. The capability of cleavage of pBR322 DNA by the complexes was investigated using agarose gel electrophoresis, and the results indicate that all complexes exhibit an efficient DNA cleavage. The cytotoxic and antiproliferative studies show that the four complexes exhibit good cytotoxic activity against different cell lines tested in general and are especially effective against Hep-G2 cell lines, and complex **4** showed IC_{50} cytotoxicity coefficients similar to those of cisplatin. Increasing the length of the carbon chain enhances the higher efficiency DNA-binding rate of cellular uptake and, consequently, the cytotoxic activity. This improvement is likely to be related with a more favorable balance between lipophilicity and hydrophilicity due to the presence of different dicarboxlate aliphatic chains bonded to palladium. All encouraging chemical and biological findings indicate that these complexes are very promising candidates as live-cell imaging reagents that could contribute to the understanding of cellular uptake of metal complexes. Further studies are warranted to assess their pharmacological properties in vivo and to elucidate the actual mechanism of their biological activity.

Acknowledgment. We gratefully acknowledge the Natural Science Foundation of China (No. 20671064, 20971090), Foundation of Educational Department of Liaoning Province (No. 20060679), Foundation of Liaoning Bai Qian Wan Talents Program (No. 2008921054), and Phenom Foundation of Liaoning colleges and universities (No. 2007R30).